# Clay Nanolayer Reinforcement of a Silicone Elastomer

Peter C. LeBaron and Thomas J. Pinnavaia*

*Department of Chemistry and Center for Fundamental Materials Research, Michigan State University, East Lansing, Michigan 48824*

*Received April 30, 2001. Revised Manuscript Received June 26, 2001*

A synthetic fluorohectorite clay in which the exchange cations have been replaced by hexadecyltrimethylammonium ions, abbreviated $C_{16}FH$, has been shown to readily intercalate linear poly(dimethylsiloxane) (PDMS) molecules containing terminal hydroxyl groups. The extent of gallery swelling increased with increasing PDMS molecular weight over the range 400−4200. Little or no intercalation was observed for PDMS molecules terminated by methyl groups, indicating that terminal silanol interactions with the gallery surfaces are an important part of the gallery swelling mechanism. These interfacial interactions may also account for the unusual correlation between the extent of gallery swelling and the molecular weight of the intercalated linear polymer. Cross-linking reactions between PDMS-4200 and tetraethyl orthosilicate in the presence of the $C_{16}FH$ organoclay afforded elastomeric nanocomposites in which the clay nanolayers were exfoliated. The nanolayer-reinforced polymer exhibited substantially improved tensile properties and resistance to swelling by an organic solvent in comparison to the pristine polymer. Also, nanolayer reinforcement greatly reduced the structural damage caused by the internal strain induced upon allowing the solvent to evaporate from the swollen polymer network. Although synthetic fluorohectorite has one of the highest nanolayer aspect ratios among smectite clays, relatively small reductions in oxygen permeability were observed for the nanocomposites. A more or less random orientation of the clay nanolayers in the polymer matrix, as indicated from TEM images of thin sectioned samples, was responsible for the lack of an effective permeant barrier.

## Introduction

As demonstrated quite convincingly in a recent review by Schollhorn,[1] the insertion of organic molecules into layered or porous inorganic hosts often results in nanocomposite materials with properties dramatically different from those of the parent end members. Nanocomposites differ from conventional composites in that the mixing of phases occurs over a much smaller length scale in comparison to the micrometer length scale of conventional composites.[2−4] When applied to the reinforcement of engineering polymers the nanocomposite concept can lead to compositions with properties far superior to conventional composites at a much reduced filler loading.

Layered-silicate clays are particularly good candidates for the nanoparticle strengthening of polymers due, in part, to their high surface area, platy morphology and exceptionally stable oxide network.[5] In certain respects the layered silicate clays share some of the same characteristics as the aerogel silicas and precipitated silicas used for the reinforcement of silicones and other polymer systems. However, in comparison to small particle silicas,[6] clays are less costly and free of health risks, adding to their attractiveness as a replacement filler for silicones. Furthermore, the rich intercalation chemistry associated with smectic clays can be used to facilitate the dispersion of the nanolayers in a polymer matrix, a feat unobtainable with conventional silica nanoparticles that tend to undergo phase-segregation in a silicone matrix.[7]

Toyota researchers were the first to demonstrate that small quantities (<10 wt %) of organoclays exfoliated in a Nylon-6 polymer matrix greatly improves the thermal, mechanical, barrier, and flame retardant properties of the polymer.[8−11] In recent years, several other polymer systems have been investigated including epoxies,[12−15] polyimides,[16−18] polyurethanes,[19] polysiloxanes,[7,20] as well as various thermoplastics.[21−30] In

(1) Schollhorn, R. *Chem. Mater.* **1996**, *8*, 1747.
(2) Messersmith, P. B.; Stupp, S. I. *J. Mater. Res.* **1992**, *7*, 2599.
(3) Okada, A.; Usuki, *A. Mater. Sci. Eng.* **1995**, *C3*, 109.
(4) Giannelis, E. P. *Adv. Mater.* **1996**, *8*, 29.
(5) Pinnavaia, T. J. *Science* **1983**, *220*, 365.
(6) Wang, Y. M. *Organosil. Mater. Appl. Chin.* **1992**, *5*, 11.
(7) Wang, S.; Li, Q.; Qi, Z. *Key Eng. Mater.* **1998**, *137*, 87.
(8) Usuki, A.; Kawasumi, M.; Kojima, Y.; Okada, A.; Kurauchi, T.; Kamigito, O. *J. Mater. Res.* **1993**, *8*, 1174.
(9) Usuki, A.; Kojima, Y.; Kawasumi, M.; Okada, A.; Fukushima, Y.; Kurauchi, T.; Kamigito, O. *J. Mater. Res.* **1993**, *8*, 1179.
(10) Kojima, Y.; Usuki, A.; Kawasumi, M.; Okada, A.; Fukushima, Y.; Kurauchi, T.; Kamigito, O. *J. Mater. Res.* **1993**, *8*, 1185.
(11) Kojima, Y.; Usuki, A.; Kawasumi, M.; Okada, A.; Kurauchi, T.; Kamigito, O. *J. Appl. Polym. Sci.* **1993**, *49*, 1259.
(12) Lan, T.; Pinnavaia, T. J. *Chem. Mater.* **1994**, *6*, 2216.
(13) Messersmith, P. B.; Giannelis, E. P. *Chem. Mater.* **1994**, *6*, 1719.
(14) Massam, J.; Pinnavaia, T. J. *Mater. Res. Soc. Symp. Proc.* **1998**, *520*, 223.
(15) Wang, Z.; Pinnavaia, T. J. *Chem. Mater.* **1998,** *10*, 1820.
(16) Yano, K.; Usuki, A.; Okada, A.; Kurauchi, T.; Kamigito, O. *J. Polym. Sci., Part A: Polym. Chem.* **1993**, *31*, 2493.
(17) Yano, K.; Usuki, A.; Okada, A. *J. Polym. Sci., Part A: Polym. Chem.* **1997**, *35*, 2289.

10.1021/cm010982m CCC: $20.00 
Published on Web 08/31/2001

earlier studies of polysiloxane−organoclay nanocomposites, dimethylditallow and hexadecyltrimethylammonium exchanged montmorillionites were dispersed in poly(dimethylsiloxane) (PDMS) with a molecular weights of 18 000 and 68 000, respectively, and cross-linked to a rubber by reaction with tetraethyl orthosilicate (TEOS). The former system afforded an exfoliated clay nanocomposite, whereas in the latter the clay was only partially exfoliated, as indicated by low-angle X-ray reflection in the final composite. Both clays, however, provided elastomer reinforcement, as well as improved thermal and solvent barrier properties.[7,20]

In an effort to elucidate the swelling of organoclay galleries by PDMS, we have examined the intercalation properties of a synthetic fluorohectorite in PDMS polymers with molecular weights in the range 400−4200. These smaller PDMS polymers make it possible to follow the gallery expansion process quantitatively by wide-angle X-ray diffraction methods. Also, the synthetic fluorohectorite used in this work has a substantially larger nanolayer aspect ratio (∼2000) in comparison to naturally occurring montmorillonite (∼200). The higher nanolayer aspect ratio should provide even better reinforcement and barrier properties, the two performance properties in need of greatest improvement for silicone rubbers. Accordingly, we also have prepared a cross-linked silicone rubber−exfoliated fluorohectorite nanocomposite and investigated its tensile strength, dioxygen permeability, and solvent uptake properties in comparison to the pristine elastomer. The results clearly demonstrate the substantial reinforcement that is possible at clay nanolayers loading of 5−10 wt %, though the permeability of the nanocomposites remains high despite the larger nanolayer aspect ratio.

## Experimental Section

**Materials.** PDMS polymers with average molecular weight values of 400, 1750, and 4200 and tin(II) 2-ethylhexaonate were obtained from Gelest, Inc. Hexadecyltrimethylammonium bromide and all other chemicals were purchased from Aldrich Chemical Co. and used without further purification.

**Organoclay Synthesis.** Lithium fluorohectorite (Corning, Inc.) with an anhydrous unit cell formula of $Li_{1.12}[Mg_{4.88}Li_{1.12}](Si_{8.00})F_4$ was ion-exchanged with a 2-fold stoichiometric excess of hexadecyltrimethylammonium bromide. A mixture of the surfactant cations and a 1.0 wt % aqueous suspension of the inorganic clay was stirred at room temperature for 12 h. The flocculated organoclay was removed by vacuum filtration and the excess surfactant was washed from the clay by resuspending the solid in water, filtering again, and then subjecting the solid to a final Soxhlet extraction in ethanol for 24 h. The clay was then dried, crushed, and sieved to a particle size <106 $\mu$m prior to use in the intercalation and nanocomposite studies. The water and organic content of the air-dried organoclay, as determined by the weight loss at 150 °C and 500 °C, was 6 and 24 wt %, respectively.

**Nanocomposites Synthesis.** A predetermined amount of organoclay was added to the desired PDMS polymer and mixed for 12 h. A stoichiometric amount of tetraethyl orthosilicate (TEOS) as a cross-linking agent and tin(II) 2-ethylhexanoate as a catalyst (TEOS:Sn = 4:1) were added to the PDMS−organoclay mixture. The resulting thixotropic mixture was then transferred to an aluminum mold and outgassed under vacuum. Cross-linking of the nanocomposite was carried out under vacuum at ambient temperature for 12 h, followed by an additional 12 h at 100 °C.

**Physical Measurements.** X-ray powder diffraction (XRD) patterns were recorded on a Rigaku rotaflex 200B diffractometer equipped with Cu Kα X-ray radiation and a curved crystal graphite monochromator. X-ray analysis of liquid PDMS polymer−organoclay mixtures were accomplished by dropping the suspension onto filter paper mounted on a glass slide with two-sided tape and blotting away the excess liquid. After the addition of TEOS and the Sn catalyst to the clay−PDMS mixture, the mixture was likewise dispersed onto a filter paper slide and the X-ray diffraction pattern was recorded during the polymerization process. Cross-linked nanocomposites were examined by mounting a rectangular flat specimen into an aluminum X-ray sample holder. After data collection, the sample was turned over to collect diffraction data from the opposite side of the casting, verifying homogeneous distribution of the clay particles. This test of homogeneous particle distribution has proven to be important in studying nanocomposites, as poorly dispersed mixtures typically lead to settling of the clay particles during polymerization. In this latter case only the bottom surface of the casting will indicate the true nature of the clay component.

Tensile measurements were made under ambient conditions according to ASTM procedure D3039 using an SFM-20 United Testing System. The dog-bone-shaped samples used in the tensile measurements were 28 mm long in the narrow region, 3 mm thick, and 3 mm wide along the center of the casting.

Oxygen permeability data were acquired on a Mocon Oxtran 2/60 oxygen permeability instrument with a test gas containing 5 vol % oxygen in nitrogen. Film samples with a thickness between 0.7 and 1.0 mm, which were cast from an aluminum disk mold, were held in the testing cells with adhesive foil masks. Pristine and nanocomposite PDMS samples were soaked in pentane until they reached a maximum uptake of solvent. The samples were then removed from the solvent and photographed after different stages of solvent evaporation to record the mechanical damage to the polymer.

TEM images were obtained on a JEOL JEM-100CX II microscope using a $CeB_6$ filament and an accelerating voltage of 120 kV. Thin-sectioned samples were prepared by embedding the PDMS nanocomposites in a glassy epoxy matrix and sectioning on an ultramicrotome. The thin sections (∼80 nm) were supported on 300 mesh nickel grids.

## Results

The organoclay used in the synthesis of nanocomposites was a hexadecyltrimethylammonium ion exchanged fluorohectorite, abbreviated $C_{16}$FH. This organo clay, which was prepared by ion exchange reaction of $Li^+$−FH, exhibited a $d_{001}$ basal spacing of 27.4 Å. Solvating the organoclay in PDMS polymers with average molecular weights in the range 400−4200 caused the basal spacing of the clay to increase. As shown by the diffraction patterns in Figure 1 the basal spacing increased with increasing chain length of the PDMS

(18) Lan, T.; Kaviratna, P. D.; Pinnavaia, T. J. *Chem. Mater.* **1994**, *6*, 573.
(19) Wang, Z.; Pinnavaia, T. J. *Chem. Mater.* **1998**, *10*, 3769.
(20) Burnside, S. D.; Giannelis, E. P. *Chem. Mater.* **1995**, *7*, 1597.
(21) Kawasumi, M.; Hasegawa, N.; Kato, M.; Usuki, A.; Okada, A. *Macromolecules* **1997**, *30*, 6333.
(22) Usuki, A.; Kato, M.; Okada, A.; Kurauchi, T. *J. Appl. Polym. Sci.* **1997**, *63*, 137.
(23) Kurokawa, Y.; Yasuda, H.; Oya, A. *J. Mater. Sci. Lett.* **1996**, *15*, 1481.
(24) Kato, M.; Usuki, A.; Okada, A. *J. Appl. Polym. Sci.* **1997**, *63*, 1781.
(25) Hasegawa, N.; Kawasumi, M.; Kato, M.; Usuki, A.; Okada, A. *J. Appl. Polym. Sci.* **1998**, *67*, 87.
(26) Porter, T, L.; Hagerman, M. E.; Reynolds, B. P.; Eastman, M. P.; Parnell, R. A. *J. Polym. Sci., Part B: Polym. Phys.* **1998**, *36*, 673.
(27) Akelah, A.; Moet, A. *J. Mater. Sci.* **1996**, *31*, 3589.
(28) Vaia, R. A.; Jandt, K. D.; Kramer, E. J.; Giannelis, E. P. *Macromolecules* **1995**, *28*, 8080.
(29) Vaia, R. A.; Jandt, K. D.; Kramer, E. J.; Giannelis, E. P. *Chem. Mater.* **1996**, *8*, 2628.
(30) Vaia, R. A.; Giannelis, E. P. *Macromolecules* **1997**, *30*, 8000.

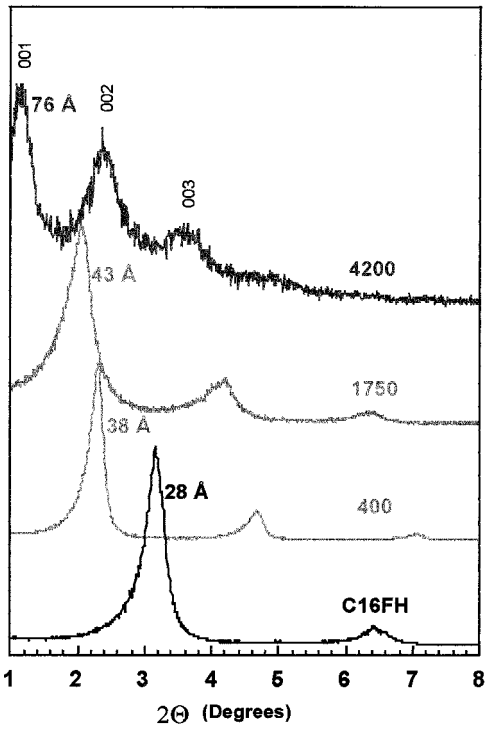


**Figure 1.** X-ray diffraction patterns of synthetic hexadecyltimethylammonium fluorohectorite, abbreviated $C_{16}FH$, intercalated by PDMS polymers with molecular weights of 400, 1750, and 4200. The pattern for the initial organo clay is included for comparison.

polymer. The PDMS with MW = 4200 gave the largest spacing (75 Å), corresponding to a gallery height of ~65 Å. Since PDMS-4200 showed the greatest tendency to swell the galleries of the organoclay, this polymer was used to form silicone rubber−organoclay nanocomposites.

Silicone rubber nanocomposites containing up to 10 wt % organoclay were prepared by cross-linking mixtures of PDMS-4200 and $C_{16}FH$ using tetraethyl orthosilicate (TEOS) as the cross-linking agent and tin(II) 2-ethylhexaonate as the catalyst. XRD patterns of a representative reaction mixture at different stages of cross-linking are shown in Figure 2. Significantly, the 002 reflection increased from 38 Å in the initial intercalate to ~50 Å after only 10 min of partial curing at 80 °C. At this incomplete stage in the cross-linking process the nanolayers have been pushed apart by the by ~90 Å. The cross-linked nanocomposite (12 h, 100 °C) showed no evidence for a 00*l* clay refection, indicating that the nanolayers were optimally exfoliated. Also, as shown by the inset in Figure 2, the clay in-plane 060 reflection near 60° 2$\theta$ was observed in the cured composite, indicating the retention of nanolayer crystallinity, even though it is highly dispersed.

Tensile data were obtained for dog-bone-shaped castings of the silicone elastomers containing 0.0, 5.0, and 10 wt % organoclay loadings. These organoclay loadings correspond to silicate loading of 0.0, 3.5, and 7.1 wt %, respectively. Figure 3 provides the stress−strain curves for each composition. Table 1 summarizes the corresponding values of tensile strength, modulus, and strain at break.

Included in Table 1 are the oxygen permeability results and cyclohexane uptake values for the pristine

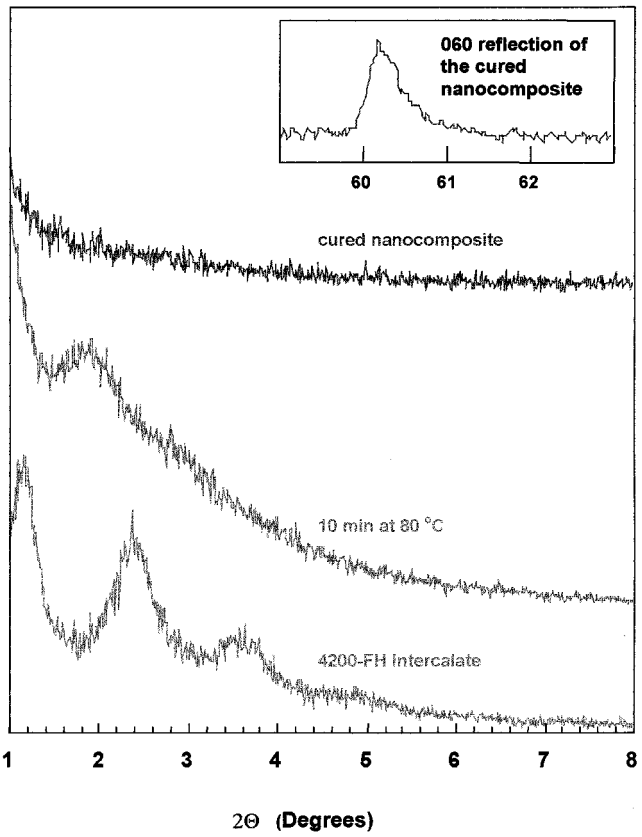


**Figure 2.** X-ray diffraction patterns of mixtures of PDMS-4200 and $C_{16}FH$ organoclay at different stages of cross-linking. The cross-linking agent was tertraethyl orthosilicate and the catalyst was tin(II) octoate. The inset indicates the presence of an in-plane 060 clay reflection in the exfoliated composite.

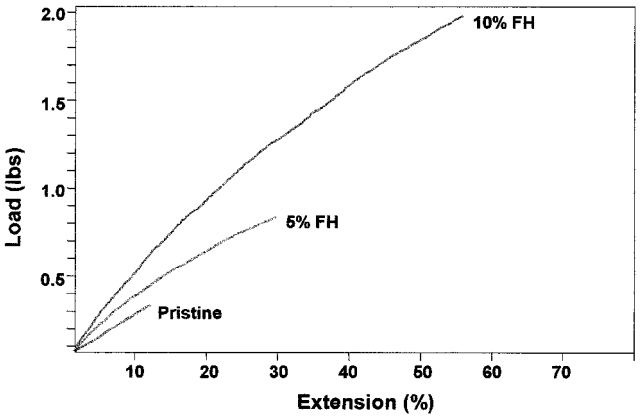


**Figure 3.** Comparison of the stress−strain curves for pristine PDMS and PDMS-$C_{16}FH$ nanocomposites containing 5.0 and 10 wt % $C_{16}FH$ organoclay.

and clay-reinforced elastomers. The permeabilities represent the transmission rates of oxygen at a concentration of 5.0% in nitrogen as a carrier gas, and the cyclohexane uptake values are the loadings of liquid solvent contained in the elastomer at equilibrium at 25 °C.

## Discussion

The replacement of $Li^+$ by hexadecyltrimethylammonium ions in the galleries of fluorohectorite resulted in a basal spacing of 27.4 Å. The difference between the observed basal spacing and the estimated clay layer

**Table 1. Properties of Silicone Elastomer[a]−$C_{16}$FH Organoclay Nanocomposites**

| organoclay loading, wt %[b] | strength, kPa | modules, kPa | elongation, % | oxygen permeability[c] | cyclohexane uptake, g/g[d] |
|---|---|---|---|---|---|
| 0.0 | 152 | $1.8 \times 10^{-3}$ | 11 | $6.12 \times 10^{4}$ | 2.55 |
| 5.0 | 361 | $2.3 \times 10^{-3}$ | 31 | | 1.07 |
| 10.0 | 880 | $3.5 \times 10^{-3}$ | 52 | | |
| 1.5 | | | | $5.75 \times 10^{4}$ | |
| 8.0 | | | | $4.56 \times 10^{4}$ | |

[a] The elastomer was formed by cross-linking PDMS (MW = 4200) a with a stoichiometric amount of TEOS. [b] The organic and water content of the clay was 6% and 24%, respectively. [c] The permeability is expressed in $cm^3$ $day^{-1}$ for a film 1.0 $m^2$ in area and one-thousandth of an inch in thickness. [d] Grams of cyclohexane/gram of polymer.

thickness (9.6 Å) indicated a gallery height of 17.8 Å. This value is consistent with a paraffin-like orientation of the surfactant chains in the gallery region. If the carbon chains adopted an all-anti conformation, the observed gallery height would correspond to an angle of inclination of ~50° between the chain axis and the clay surface. However, the chains are most likely kinked[31] and oriented more vertically on the gallery surfaces. Ordinarily, long-chain ammonium ion surfactants adopt lateral bilayer to pseudotrimolecular orientation in the gallery space of montmorillonite, resulting in gallery heights below 10 Å.[31−33] However, synthetic fluorohectorite has a higher layer charge (1.12 e− per $O_{20}$ per unit cell) in comparison to montmorillonite, which usually has a layer charge density of ~0.75 e− per $O_{20}$ per unit cell. Thus, the higher population of surfactant chains in fluorohectorite result in a paraffin-like packing of chains and a comparatively large gallery expansion.

Somewhat surprisingly, the extent of clay gallery expansion upon PDMS intercalation is dependent on the molecular weight of the guest polymer (cf., Figure 1). This is not the usual outcome observed when other linear molecules are intercalated into an organoclay. Ordinarily, the gallery height is determined by the orientation of organocation in the gallery and the critical diameter of the intercalated polymer. The length of the guest species usually has little or no effect on the gallery height. That is, the organoclay normally permits a fixed volume of the prepolymer to intercalate as dictated primarily by the polarity match between the linear polymer, gallery surface, and gallery cation. The gallery heights observed in the PDMS−fluorohectorite systems, however, are determined by the molecular weight or, equivalently, the ratio of $-OSi(CH_3)_2-$ repeat units to terminal $-Si(CH_3)_2OH$ groups. As this ratio increases, the gallery height increases.

The hydrophobicity of the organocation surfactant undoubtedly plays an important role in allowing the initial penetration of PDMS into the galleries. However, the silanol end groups of the polymer interact at least in part with the gallery surfaces. These interactions most likely play a role in determining the space-filling configuration of the PDMS. The importance of specific interactions between the silanol end groups and the gallery surfaces is verified by the observation that PDMS polymers of the same molecular weight but terminated exclusively by methyl groups do not intercalate into $C_{16}$FH. As illustrated schematically in Figure 4, restricting the silanol end groups to specific contacts with the gallery surface will influence the packing of long-chain PDMS molecules (e.g., PDMS-4200) in the gallery. Shorter PDMS chains that are comparable in length to the organocation (e.g., PDMS-400, which contains ~6 $-Si(CH_3)_2O-$ units) cannot bridge opposite gallery surfaces and at the same time account for a 10 Å or more increase in gallery height in comparison to $C_{16}$FH (e.g., compare the diffraction patterns in Figure 1). Thus, in the case of short PDMS chains only one terminal silanol group may be linked to the gallery surface.

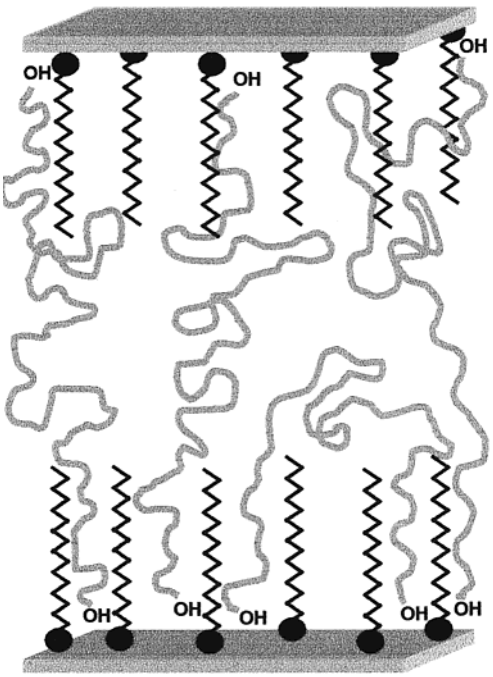


**Figure 4.** Schematic representation of the swelling of an alkylammonium ion exchanged fluorohectorite by a long-chain PDMS polymer (MW = 4200) containing terminal OH groups. Shorter PDMS chains with molecular weight fractions of 400 and 1750 may have only one end of the chain associated with the gallery surfaces.

The charged headgroups of the surfactant, the siloxane oxygens of the clay layer, and coadsorbed water molecules may all contribute to the interactions of the terminal silanol groups with the gallery surfaces. Burnside and Giannelis have noted that a small amount of gallery water was needed to intercalate a PDMS-18 000 polymer into an organo montmorillonite. We have verified the need for gallery water to achieve PDMS intercalation. The air-dried organoclay used in the present work contained ~6 wt % water, as judged by the weight loss upon drying at 150 °C, but if the water is removed by drying at elevated temperatures, then no PDMS intercalation was observed. In view of these results, it is now clear that water is needed to facilitate interaction of the terminal silanols and the gallery surfaces, presumably through hydrogen bond formation. Once the H-bonding sites are saturated, PDMS intercalation is complete and there is no further swelling of the clay galleries.

(31) Legaly, G. *Solid State Ionics* **1986**, *22*, 43.
(32) Hackett, E., Manias, E., Gianellis, E. P. *J. Chem. Phys.* **1998**, *108*, 7410.
(33) Teppen, B. J.; Rasmussen, K.; Bertsch, P. M.; Miller, D. M.; Schafer, L. *J. Phys. Chem. B* **1997**, *101*, 1579.

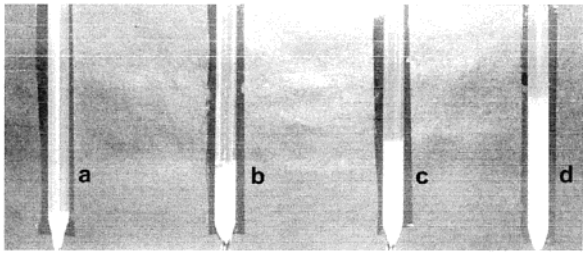


**Figure 5.** Photograph of PDMS polymer−$C_{16}$FH organoclay mixtures containing 5.0 wt % organoclay and equilibrated at room temperature. The mixtures were formed from (a) methyl-terminated PDMS-400, (b) OH-terminated PDMS-400, (c) OH-terminated PDMS-1750, and (d) OH-terminated PDMS-4200.

Although the swelling of $C_{16}$FH is best monitored quantitatively by XRD, the dependence PDMS intercalation on molecular weight can be qualitatively judged by the physical behavior of the clay in PDMS suspensions. Figure 5 is a photograph of four different $C_{16}$FH−PDMS suspensions, each containing 5 wt % organoclay. The tubes are filled from left to right order with methyl-terminated PDMS-400 and silanol-terminated PDMS-400, -1750, and -4200. The methyl-terminated PDMS does not intercalate into the galleries, and the unexpanded clay settles to the bottom of the tube. For the silanol-terminated PDMS derivatives, however, the nanolayers are separated by PDMS molecules, allowing for the formation of a stable, scaffoldlike suspension of swollen clay tactoids with an equilibrium height that increases with the PDMS polymer molecular weight.

The Sn(II)-catalyzed cross-linking of PDMS-4200 by TEOS in the presence $C_{16}$FH organoclay leads to further expansion of the galleries and the formation of silicone rubber−clay nanocomposite (cf., Figure 2). The absence of an observable 001 diffraction peak in the cured elastomer implies that the clay nanolayers have been optimally separated (exfoliated) by the elastomer matrix. This means that the intragallery cross-linking rate was competitive with the extra gallery rate. For this to occur the catalyst and TEOS should be favorably partitioned between the PDMS solution and the organoclay galleries. Coadsorbed water may also facilitate intragallery polymerization through TEOS hydrolysis. Verification that the individual clay nanolayers retained their structural integrity in the exfoliation process was provided by the presence of a 060 in-plane reflection in the high $2\theta$ region near 60° (see inset in Figure 2).

The uniform dispersion of clay nanolayers in the nanocomposite affords a marked improvement in the tensile strength, modulus, and strain-at-break (see Figure 3 and Table 1). Similar improvements in tensile properties have been reported for silicone rubber−clay nanocomposites derived from PDMS polymers with molecular weights of 18 000 and 68 000.[7,20] Through the absorption and dispersal of an applied load, the nanolayers layers delocalize stress, as well as toughen the matrix as indicated by the large increase in the strain-at-break. In contrast, conventional composites ordinarily compromise toughness for tensile strength. It has been previously noted[14,20] that the clay nanolayer reinforcement of elastomers dramatically reduces the ability of the matrix to absorb solvents. An analogous reduction in cyclohexane uptake was observed for the clay nanolayer reinforced silicone elastomers prepared in the present work (cf., Table 1). However, the reinforcement effect goes far beyond simply limiting the uptake of solvent. The clay nanolayers can also dramatically reduce the structural damage that normally occurs when the solvent is allowed to evaporate from a solvent-saturated elastomer. As shown in Figure 6, the rapid evaporation of cyclohexane from the pristine silicone rubber causes internal strain that fractures the matrix, rendering the recovered elastomer useless. In contrast, the nanolayer-reinforced composite undergoes less solvent swelling and loses solvent more slowly, thus reducing internal strain and avoiding matrix fracture. The avoidance of structural damage caused upon expo-

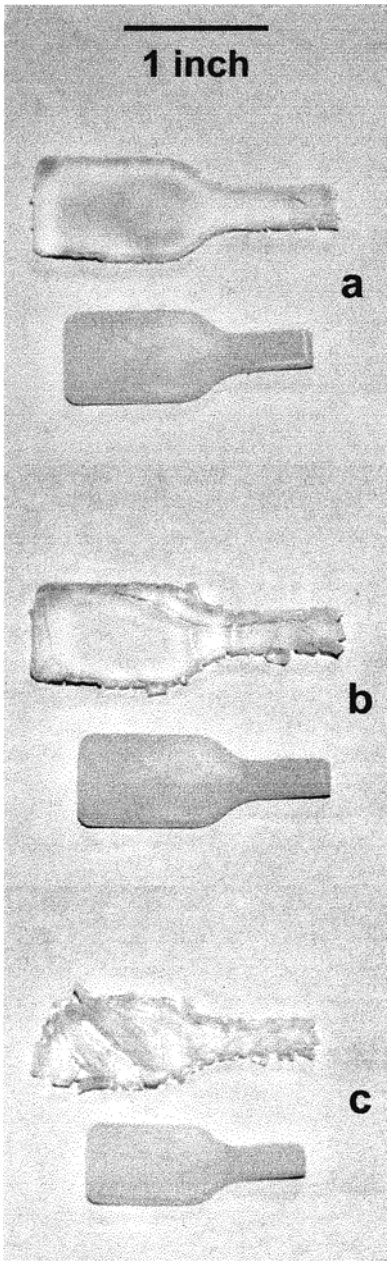


**Figure 6.** Photographs of a pristine silicone elastomer formed from PDMS-4200 (upper specimen) and the corresponding nanocomposite containing 5.0 wt % $C_{16}$FH organoclay (lower specimen) after equilibration in a cyclohexane bath and subsequent removal from the bath to allow for solvent evaporation: (a) immediately after removal from the bath, (**b**) after 15 s, and (**c**) after 20 min. No structural damage was noted for the nanocomposite after complete evaporation of the solvent.

sure to solvents may represent one of the most important benefits of nanolayer reinforcement in elastomeric polymer technology.

Although the tensile and solvent resistance properties of a silicone rubber can be greatly enhanced through clay nanolayer reinforcement, the gas permeability of the nanocomposites was only slightly affected. Even at an organoclay loading of 8.0 wt % organoclay, the oxygen permeability was only reduced only by ~25% (see Table 1). In contrast, previous work has shown that dramatic reductions in permeability can be achieved for polyimide films and other thin film forms of polymers.[34−38] For instance, the exfoliation of 2 wt % synthetic mica in a polyimide film reduced the water vapor permeability 10-fold,[37] and a 4.8 wt % dispersion of clay in poly($\epsilon$-caprolactone) reduced the water vapor permeability 5-fold.[35]

In general, a reduction in the permeability of a nanolayer-reinforced polymer film can be anticipated if the nanolayers are highly aligned parallel to the film surfaces or if the constrained polymer region near the clay interface is large.[39] Aligned nanolayers increase the tortuosity of the diffusion path, causing the permeability to decrease with increasing aspect ratio of the nanolayers. A thick constrained polymer region can also reduce the permeability by decreasing both the diffusion rate and the solubility of the permeant. Although synthetic fluorohectorite has one of highest nanolayer aspect ratios among smectite clays, it has not been effective in providing substantially reduced gas permeability in the case of silicone elastomers. This suggests that the nanolayers are not well aligned or that the constrained polymer region is relatively thin. Under the conditions used to form sufficiently thick samples for the permeability measurements, the surface tension forces are too weak to facilitate nanolayer ordering parallel to the sample surface. The relatively random orientation of the nanolayers was verified by transmission electron microscopy. As shown by the lower TEM image in Figure 7, the nanolayers generated by the exfoliation of a clay tactoid tend to orient parallel to one another. However, as shown by the upper image in Figure 7, wherein nanolayers emanating from different tactoids are nearly orthogonal to each other, there is little or no tendency for the nanolayers to orient uniformly through out the matrix. Thus, better methods for achieving nanolayer orientation must be devised if substantially reduced permeability is to be achieved for silicone−clay nanocomposites through a tortuous path mechanism. It appears that a constrained polymer region does not play an important role in reducing the permeability of the nanocomposite.

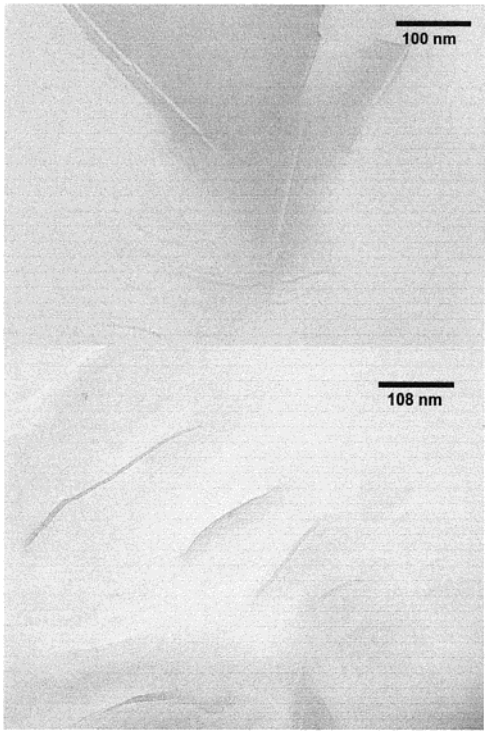


**Figure 7.** TEM images of a cross-linked silicone elastomer prepared from PDMS-4200 and 10 wt % $C_{16}$FH organoclay.

**Acknowledgment.** This work has been supported in part by the Center for Fundamental Materials Research and the Composite Materials and Structure Center at Michigan State University.

CM010982M

(34) Messersmith, P. B.; Gianellis, E. P. *Chem. Mater.* **1993**, *5*, 1064.
(35) Messersmith, P. B.; Gianellis, E. P. *J. Polym. Sci. Part A: Polym. Chem.* **1995**, *33*, 1047.
(36) Yano, K.; Usuki, A.; Okada, A.; Kurauchi, T.; Kamigaito, O. *J. Polym. Sci. Part A: Polym. Chem.* **1993**, *31*, 2493.
(37) Yano, K.; Usuki, A.; Okada, A. *J. Polym. Sci. Part A: Polym. Chem.* **1997**, *35*, 2289.
(38) Kojima, Y.; Usuki, A.; Kawasumi, M.; Okada, A.; Kurauchi, T.; Kamigaito, O. *J. Appl. Polym. Sci.* **1993**, *49*, 1259.
(39) Beall, G. In *Polymer−Clay Nanocomposites*, Pinnavaia, T. J., Beall, G. W., Eds.; Wiley: New York, 2000; pp 267−277.